J Mater Sci (2007) 42:7977–7980
DOI 10.1007/s10853-007-1886-1

LETTER

A model to explain extensive superplasticity in polycrystalline materials

Yan Dong · Zhonghua Li · Jun Sun

Received: 15 May 2007 / Accepted: 25 May 2007 / Published online: 30 June 2007

Superplastic behavior has been observed in a variety of metallic systems during high temperature deformation. The possibility of superplastic flow in nanocrystalline materials at low temperatures is reported in molecular-dynamics simulations [1, 2] and in experimental evidences [3–6]. Karch et al. [3] observed that conventional brittle ceramics became ductile at low temperature if a polycrystalline ceramics was generated with a crystal size of a few nm. Lu et al. [4] showed recently that bulk, highly pure nanocrystalline copper could be strained at room temperature by up to 5,000% without strain hardening and changing grain size. These experimental results indicate that conventional dislocation mechanisms are not responsible for the large strain and that the extensive superplasticity seems to originate from grain boundary (GB) diffusion (Coble creep). This novel behavior, however, could not be explained by present models and theories.

Lee [7] proposed a model to show grain rearrangement process by Coble creep and GB migration, which is shown in Fig. 1 from *a* to *e*. The model consists of hexagonal single-phase grains of uniform size and shape loaded in tension (Fig. 1a). On first loading, the GB diffusion fluxes flow (see Fig. 2a) causing the grains to elongate along the stress axis (Fig. 1b). At a strain $\varepsilon = 0.55$, the grains become diamond-shaped (Fig. 1c). At this point the four-grain junctions become unstable. GB migration (with no additional strain) will return the diamond-shaped grain to initial one, and switch grain neighbors with a rotation of 30° (Fig. 1e). The Lee model shows a plausible way to switch grain neighbors, resulting in a strain $\varepsilon = 0.55$ while retaining the equiaxed grain structure. However, Lee model fails to give a reasonable physical path for a continuous elongation beyond the 55% strain, and therefore can not be used to explain extensive superplasticity. To go beyond the first grain switching event and account for the existence of a sequence of such switching events we look at the microstructure tilted by 30° (or –30°) as shown in a'. Although the grain structure after first grain switching (Fig. 1e) is a "dead end" for the model operating along the vertical direction, the grain structure in the tilted direction is equivalent to *a*. Therefore, the Lee model can operate in the slant loading direction as described by several representative steps a', b' and e', corresponding to steps *a*, *b* and *e*, respectively. At step e', the arrangement of grains returns to initial one as shown in Fig. 1a, but switches their neighbors with a resulting strain $\varepsilon = 1.0$. Evidently, after step e' the deformation process shown in Fig. 1 from steps *a* to e' can always repeat during loading. If the model operates *n*-cycles in observation time, obvious superplasticity of $n \times 100\%$ occurs.

Thus, the extended Lee model gives a reasonable physical path for explaining the extensive superplasticity observed in polycrystalline materials. However, whether there is an obvious superplasticity for the materials depends on how fast the model operates one cycle (from *a* to e' in Fig. 1).

Lee made no attempt to develop a solution for his model. Spingarn and Nix [8] made a solution for Lee model having not yet deformed (the model shown in Fig. 1a). This

Y. Dong · Z. Li (✉)
Department of Engineering Mechanics, Shanghai Jiaotong University, Shanghai 200240, P.R. China
e-mail: zhli@sjtu.edu.cn

J. Sun
State Key Laboratory for Mechanical Behavior of Materials, School of Materials Science and Engineering, Xi'an Jiaotong University, 710049 Xi'an, P.R. China

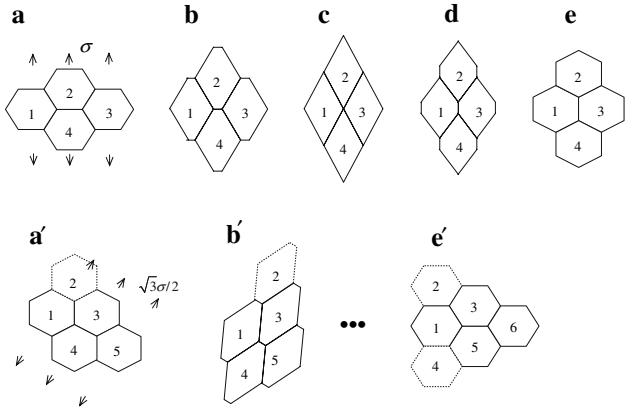

Fig. 1 The extended Lee model: The steps from *a* to *e* describe the original Lee model, and the steps from *a′* to *e′* indicates the operation of Lee model in a slant loading direction. *a*, initial state. *b*, intermediate state during grain boundary diffusion. *c*, critical position with a strain ε = 0.55. *d*, intermediate state during grain boundary migration without additional strain. *e*, final state of the Lee model, switching grain neighbors and leading to a strain ε = 0.55. *a′*, in a slant loading direction (30° with respect to applied stress) the array of grains 1, 3, 4, 5 is equivalent to *a*, then the steps from *a* to *e* can repeat in the slant direction. *b′*, intermediate state during grain boundary diffusion. *e′*, final state of the extended Lee model. In this step, grain 1 inserts into grains 2 and 4 leading to a strain ε = 1.0, and returning the grain array (see grains 1, 3, 5, 6) to the initial state as shown in *a*. Then the model can repeat itself during loading to produce large strain

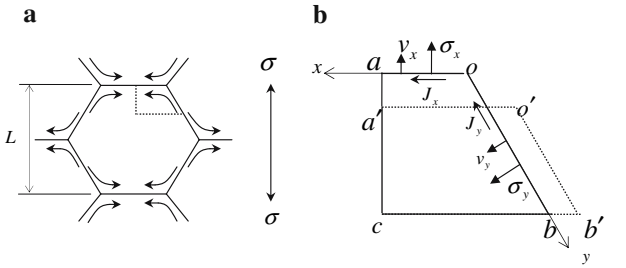

Fig. 2 The analytical model: *a*, the atom fluxes along grain boundaries. The area closed by dotted lines and grain boundaries denotes a representative cell. *b*, the coordinate system and deformation behavior of the cell during loading. The dimension of the cell is normalized by grain size *L*, the grain boundary length $a = b = \sqrt{3}/6$ at initial state (not yet deformed), and $a = 0$, $b = \sqrt{15}/6$ at the critical state (see Fig. 1c). The area of the cell keeps constant during deformation, which is equal to $\sqrt{3}/96$

solution is similar to other models [9, 10], approximately applies for infinitesimal strain. The strain rate for the finite strain of the model is also proposed by Spingarn and Nix as a function of strain. However, their solution is valid up to a strain ε = 0.55, and is difficult for practical use because the strain itself is unknown. A complete solution, which satisfies both compatibility (grain continuity) and stress boundary conditions, and tracks the whole deformation procedure of the Lee model, is given here.

As shown in Fig. 2a, only a representative unit cell needs to be considered due to periodic symmetry, which is shown in Fig. 2b. The initial shape of the cell (not yet deformed) is denoted by $cb'o'a'$. Symmetry requires that the grain boundaries (GBs) keep straight line and move parallel during deformation such that the current shape of the cell is described by *cboa*. The dimension of the cell in Fig. 2b is normalized by grain size *L*. Setting moving coordinates *x* and *y* on the horizontal and inclined boundaries, with original point at the boundary junction *o*, the atomic fluxes along GBs are given by

$$J_x = \frac{\Omega\delta_b D_b}{kT}\frac{\partial\sigma_x}{L\partial x}, \quad J_y = \frac{\Omega\delta_b D_b}{kT}\frac{\partial\sigma_y}{L\partial y} \tag{1}$$

where D_b is the GB diffusivity, δ_b the GB thickness, Ω the atomic volume, kT has the usual meaning, σ_x and σ_y are, respectively, the normal tractions on *x* and *y*, positive for tension and negative for compression.

The conservation of matter requires that $\partial J_x/L\partial x + v_x = 0$, $\partial J_y/L\partial y + v_y = 0$, where v_x and v_y are the rate of accumulation or depletion of matter on GBs, positive for accumulation and negative for depletion. Thus, we have

$$\frac{\Omega\delta_b D_b\partial^2\sigma_x}{kTL^2\partial x^2} + v_x = 0, \quad \frac{\Omega\delta_b D_b\partial^2\sigma_y}{kTL^2\partial y^2} + v_y = 0 \tag{2}$$

The quantities in the analyses are normalized as follows

$$\overline{\sigma}_x = \sigma_x/\sigma, \overline{\sigma}_y = \sigma_y/\sigma, \quad \overline{t} = \frac{\sigma\delta_b D_b\Omega}{kTL^3}t, \quad \overline{v} = \frac{kTL^2}{\sigma\delta_b D_b\Omega}v \tag{3}$$

where σ is the applied stress, $\overline{t}$ is the normalized time. Thus, Eq. 2 can be rewritten as

$$\frac{\partial^2\overline{\sigma}_x}{\partial x^2} + \overline{v}_x = 0, \quad \frac{\partial^2\overline{\sigma}_y}{\partial y^2} + \overline{v}_y = 0 \tag{4}$$

Integrating Eq. 4 yields

$$\overline{\sigma}_x = -\frac{1}{2}\overline{v}_x x^2 + C_1 x + C_2, \quad \overline{\sigma}_y = -\frac{1}{2}\overline{v}_y y^2 + C_3 y + C_4 \tag{5}$$

The parameters, $\overline{v}_x, \overline{v}_y, C_1, C_2, C_3, C_4$, can be determined from the following boundary conditions:

(a) Symmetry requires that the fluxes at $x = a$ and $y = b$ must be zero at every time. Hence $C_1 = a\overline{v}_x, C_3 = b\overline{v}_y$.

(b) Conservation of matter implies that the outflow and inflow of atoms at the junction *o* must be equal, i.e., J_x $(x = 0) + 2J_y$ $(y = 0) = 0$, then we have $C_1 = -2C_3$, and therefore $b\overline{v}_y = -a\overline{v}_x/2$.

(c) Continuity of chemical potential implies that the stresses at the junction o must be equal. Hence $C_2 = C_4$.

(d) The average normal stress along the inclined GB is zero [8, 11], that is, $\int_0^b \overline{\sigma}_y dy = 0$, which leads to $C_4 = -b^2\overline{v}_y/3$.

(e) The force equilibrium condition $\int_0^a \overline{\sigma}_x dx = \sqrt{3}/4$ yields $a^2\overline{v}_x(a + b/2) = 3\sqrt{3}/4$. Using this equation, together with the current area of the cell given by $\sqrt{3}b(a + b/4)/2 = 5\sqrt{3}/96$ leads to

$$\overline{v}_x\left(\frac{125}{1728b^3} - \frac{25}{144b} - \frac{5}{12}b + b^3\right) = 48\sqrt{3} \tag{6}$$

When the grains have not yet deformed, as considered by Spingarn and Nix [8], $b = \sqrt{3}/6$, we have $\overline{v}_x = 36$. Recalling that $v_x = \overline{v}_x(\sigma\delta_b D_b \Omega/kTL^2)$ leads to $v_x = 36\sigma\ \delta_b\ D_b\ \Omega\ /kTL^2$. The strain rate is then given by $\dot{\varepsilon} = v_x/L = 36\sigma\delta_b D_b\Omega/kTL^3$. This is just the result obtained by Spingarn and Nix.

The $\overline{v}_x$ in Eq. 6 can be expressed as $\overline{v}_x = \frac{\sqrt{3}}{2}\frac{db}{d\overline{t}}$. Hence

$$\frac{db}{d\overline{t}}\left(\frac{125}{1728b^3} - \frac{25}{144b} - \frac{5}{12}b + b^3\right) = 96 \tag{7}$$

Equation 7 is valid in the range of $b \in [\sqrt{3}/6, \sqrt{15}/6]$. Integrating Eq. 7 from $b = \sqrt{3}/6$ to b yields

$$-\frac{125}{864b^2} - \frac{25}{36}\ln b - \frac{5}{6}b^2 + b^4 + 0.9358 = 384\overline{t}. \tag{8}$$

Equation 8 indicates that the normalized time $\overline{t}$ corresponds to a certain configuration of the deformed model, for instance, $\overline{t} = 0, b = \sqrt{3}/6$, describing initial shape of the grain (Fig. 1a); when $\overline{t} = 0.00187, b = \sqrt{15}/6$, the grain becomes diamond-shaped (Fig. 1c).

The driven force for steps c to e in Fig. 1 is capillarity [12]. The GB migrates to decrease the area of the GB. Thus, the GB migration occurs spontaneously and is expected to be faster, so that the rate from stages a to e is controlled by the GB diffusion [8]. Neglecting the time spent by the GB migration, the time consumed during the deformation from steps a to e shown in Fig. 1 is given by $t_{a\text{-}e} = 0.00187kTL^3/(\sigma\ \delta_b\ D_b\ \Omega)$. The same technique may be employed to evaluate the time from steps a' to e' for the model in biaxial tensions. According to Spingarn and Nix [8], the shear stresses on the GBs are relaxed by GB sliding during creep. Using appropriate force equilibrium conditions and neglecting effect of shear stress, the time consumed from steps a' to e' is given by $t_{a'-e'} = 0.00333kTL^3/(\sigma\delta_b D_b\Omega)$. Thus, the time consumed by one cycle is

$$t_{\text{cycle}} = 0.0052\frac{kTL^3}{\sigma\delta_b D_b\Omega}. \tag{9}$$

The average strain rate in one cycle is given by $1/t_{\text{cycle}}$ because the strain in one cycle is equal to 1. Hence

$$\overline{\dot{\varepsilon}} \approx 192\frac{\sigma\delta_b D_b\Omega}{kTL^3}. \tag{10}$$

This equation predicts strain rate is much faster than the model of infinitesimal strain [8–10], indicating that the deformation mechanism of Lee model is energetically favorable.

It should be noted that the existing classical models only predict the strain rate under a condition of steady state for infinitesimal deformation. Since the atom fluxes change continuously as the grain shape changes, no real steady process is ever achieved. The present solution can describe the strain rate at any deformation stage. The model is formally applicable to perfectly regular hexagon grains during Coble creep. However, the real material contains different grain sizes and irregular grain array. It is expected that each grain in the real materials will deform in a similar manner because the deformation is controlled by the same mechanism. For the real materials of average grain size L, the individual grains will deform at different stage in order to maintain grain continuity, which leads to an average strain rate described by Eq. 10.

The rate predicted by Eq. 10 is close to that of the GBS (grain boundary sliding) accommodated model proposed by Wang [13]. Although experimental data for various metals and ceramics exhibit scattering, most of them are in good agreement with the prediction of the GBS model [13], and therefore agree with Eq. 10 as well. However, the GBS model cannot repeat itself [14], therefore does not apply for large strain.

One of the recurring questions in superplasticity behavior is the manner by which the polycrystalline aggregate as a whole deforms plastically without changing grain size, especially when an elongation of 5,000% was observed in nanocrystalline copper at room temperature [4]. Because of the size of a frank-Read source can not exceed the grain size, L, and the stress to activate such sources increases inversely with decreasing grain size ($L\sim 1/\sigma$), these sources are difficult to be activated in nanocrystalline materials [2, 15]. Hence, the conventional dislocation mechanism ceases to be operational in nanocrystalline materials, and GB diffusion dominates the supperplasticity behavior of the nanocrystalline materials. At present, it is very difficult to envision any other means to allow extensive superplasticity while retaining the equiaxed grain structure. The extended Lee model gives a

vivid description on the deformation and appears to be only one way for diffusionally accommodated grain rearrangement to produce extensive superplasticity in polycrystalline materials. Though the extension is small, it is this extension enables the Lee model to answer this question. Grain switching has been directly observed in a transmission electron microscope study of superplastic AL–Zn alloys [16], in a simulation of oil-emulsion [17] and in a finite element simulation of diffusion creep in two-dimensional polycrystalline solids [18]. In addition, the model also describes other microstructural features observed during supperplastic deformation, such as grain elongation and grain rotation [6, 18, 19].

Even though the extended Lee model could repeatedly switch grain neighbors such that infinitely lager strain could be produced in theory, other possible deformation mechanisms, such as grain sliding and lattice diffusion, could not be ruled out in practical materials. They might not be dominant, but affects, more or less, the operating of the extended Lee model. In addition, some care should be taken with the irregular grain array, e.g. grain growth accompanied by shrinkage and annihilation of small grains [18]. All these indicate that supperplastic behavior is extremely complex. However, the present model, at the first time, physically demonstrates that the extensive supperplasticity in polycrystalline materials may occur by repeatedly switching grain neighbors during Coble creep.

Acknowledgments This work was supported by the National Science Foundation of China under Grant No.10572088 and the National Basic Research Program of China through Grant No. 2004CB619303.

References

1. Schiotz J, Tolla FD, Jacobsen KW (1998) Nature 391:561
2. Yamakov V, Wolf D, Phillpot RR, Gleider H (2002) Acta Mater 50:61
3. Karch J, Birringer R, Gleider H (1987) Nature 330:556
4. Lu L, Sui ML, Lu K (2000) Science 287:1463
5. Chinh NQ, Szommer P, Horita Z, Langdon TG (2006) Adv Mater 18:34
6. Xu X, Nishimura T, Hirosaki N, Xie RJ, Yamamoto Y, Tanaka H (2006) Acta Mater 54:255
7. Lee D (1970) Metall Trans 1:309
8. Spingarn JR, Nix WD (1978) Acta Metall 26:1389
9. Coble RL (1963) J Appl Phys 34:1679
10. Green HW (1970) J Appl Phys 41:3899
11. Kitimura T, Ohtani R, Yamanaka T, Hattori Y (1995) JSME Int J 38:581
12. Suo Z (1997) Adv Appl Mech 33:194
13. Wang JN (2000) Acta Metall 48:1517
14. Yang W, Ma X, Wang H, Hong W (2004) Key Eng Mater 274–276:51
15. Rodriguez AD, Garcia DG, Solvas EZ, Shen J, Chaim R (2007) Scripta Materialia 56:89
16. Naziri H, Pearce R, Brown MH, Hale VF (1973) J Microsc 97:229
17. Ashby MF, Verrall R (1973) Acta Metall 21:149
18. Kim BN, Hiraga K (2000) Acta Mater 48:4151
19. Ford JM, Wheeler J, Movchan AB (2000) Acta Mater 50:3941